Mathematical Models and Methods in Applied Sciences
Vol. 18, No. 11 (2008) 1845–1867

World Scientific
www.worldscientific.com

MODAL MODELLING OF THE NONLINEAR RESONANT FLUID SLOSHING IN A RECTANGULAR TANK II: SECONDARY RESONANCE

MARTIN HERMANN

Institut für Angewandte Mathematik,
Friedrich-Schiller-Universität Jena,
Ernst-Abbe-Platz 1-2, Jena, 07745, Germany
hermann@mathematik.uni-jena.de

ALEXANDER TIMOKHA*

Centre for Ships and Ocean Structures,
Norwegian University of Sciences and Technology,
7091, Trondheim, Norway
alexander.timokha@ntnu.no

Received 19 February 2007
Revised 5 February 2008
Communicated by K. R. Rajagopal

In Part I of this work [*Math. Mod. Meth. Appl. Sci.* **15** (2005) 1431–1458], we studied periodic (steady-state) solutions of an asymptotic nonlinear modal system which describes two-dimensional resonant sloshing in a rectangular tank. The system was derived by Faltinsen *et al.* (2000) under the assumption that the primary excited (lowest) natural mode gives the largest contribution to the wave patterns. We found that this assumption is not true in a certain frequency domain due to internal (secondary) resonance leading to an amplification of the second mode. This frequency domain can also be identified for the critical depth-to-breath ratio $h = 0.3368\ldots$ which was discussed in Part I. In Part II, this secondary resonance is modelled by a double-dominant modal system by Faltinsen and Timokha (2001). A comparative analysis with the results from Part I is presented. The emphasis is placed on the case of the mentioned critical ratio when a double turning point arises in the branching diagram. The appearance of the double turning point explains why classical laboratory experiments by Fultz (1962) underestimate the value of the critical depth.

Keywords: Fluid sloshing; modal systems; resonant waves; bifurcations; steady solutions.

AMS Subject Classification: 76B15, 34B60, 37M20

*Permanent Address: Institute of Mathematics, National Academy of Sciences, Tereschenkivska 3, str., 01601, Kiev, Ukraine.

1. Introduction

In Part I of this work,[16] we presented an extensive survey on mathematical and numerical aspects of the nonlinear liquid sloshing in a rigid tank. Steady-state (periodic) resonant wave regimes were emphasized as those which are not unique for certain input parameters. We discussed difficulties which arise when bifurcations of these regimes are analyzed by Computational Fluid Dynamics (CDF) methods. To the authors' knowledge, the only alternative to CDF is to use an *asymptotic modal* technique which represents a subclass of the so-called *multimodal methods*.

The multimodal methods are typically used to solve the free boundary value problem formulated with respect to the velocity potential. It is assumed that the liquid is incompressible, perfect and characterized by irrotational flow. Discussions on the applicability of this physical model are, for instance, presented in monographs by Abramson[1] and Ibrahim.[17] In Part I we remarked that the physical model adequately describes sloshing of Liquefied Natural Gas (LNG), oil and other relevant liquids, whereas viscosity, surface tension, flow separation and other specific features of the contained liquids play a secondary role. They are only of interest in specific cases when, for instance, the liquid is shallow or vorticities are shed at sharp edges of structures which submerge into the liquid.

The multimodal methods reduce the original free boundary problem to a system of ordinary differential equations (*modal systems*), which couple the generalized Fourier coefficients (*modal functions* $\beta_i(t)$) in the normal representation of the free surface $\Sigma(t)$:

$$z = f(x, y, t), \quad \text{where } f(x, y, t) = \sum_{i=1}^{\infty} \beta_i(t) f_i(x, y). \tag{1.1}$$

Here $\{f_i(x, y)\}$ ($f_i = f_i(x)$ for a two-dimensional sloshing) imply the natural sloshing modes.

A truncation of the multimodal systems (with respect to $\beta_i(t)$) is needed for practical use. This reduction can be accomplished by a naive truncation of the sum in the expression (1.1) which will obviously lead to finite-dimensional modal systems (see the description of the corresponding Perko[26,30] multimodal technique in Part I). Following the Perko-like technique, we must recognize that all the nonlinear expressions containing lower as well as higher natural modes (modal functions β_i) give a comparable contribution to the liquid sloshing dynamics. This technique has extensively been elaborated in recent publications by Ferrant and Le Touze,[11] La Rocca *et al.*,[18–20] and Shankar and Kidambi.[31] The dimension of the corresponding modal systems is rather large. The systems are typically employed to solve the Cauchy problem, i.e. to simulate a nonlinear transient surface wave. Numerical aspects of these simulations, e.g. stiffness, robustness and requirement in linear damping terms, are, for instance, discussed by La Rocca *et al.*[19,20] Because of their large dimension, these multimodal systems are not appropriate for analytical studies.

Part I shows that a simplification and a related truncation of the nonlinear infinite-dimensional modal systems are also possible if we recall that the higher modes give a higher-order asymptotic contribution to the sloshing relative to that by the lowest modes. In terms of the infinite sum (1.1) this means that the modal systems may, from the asymptotic point of view, contain unnecessary quantities associated with nonlinearities in the higher modal functions $\beta_i(t)$. In order to account for this *asymptotic* fact, we should introduce an intermodal relation between the $\beta_i(t)$ and distinguish leading and driven modal modes, which cause lowest- and higher-order contributions, respectively. The procedure suggests to associate with the highest-order contribution a small non-dimensional parameter δ and to neglect the $o(\delta)$-terms. Thus, the multimodal systems are reduced to small-dimensional systems of nonlinear ordinary differential equations, namely, to *asymptotic modal systems*. The latter systems can be studied both analytically and numerically. An example is given by Faltinsen *et al.*[8] for the case of two-dimensional sloshing in a rectangular tank. The adopted intermodal ordering is as follows

$$\beta_1 = O(\delta^{1/3}); \quad \beta_2 = O(\delta^{2/3}); \quad \beta_i \leq O(\delta), \quad i \geq 3. \tag{1.2}$$

Moiseyev[24] proved that the relation (1.2) is a necessary solvability condition for a certain class of steady-state sloshing with a finite liquid depth. The (1.2)-based asymptotic modal system couples nonlinearly the two leading modal functions $\beta_1(t)$ and $\beta_2(t)$.

In Part I we have presented a bifurcation analysis of the steady-state solutions of the system by Faltinsen *et al.*[8] Here, the main focus was laid on lateral harmonic excitations of the tank so that $\delta \sim \tau$, where τ is the non-dimensional forcing amplitude. From a mathematical point of view, the steady-state solutions are associated with a two-point boundary problem using periodic boundary conditions. We showed that this problem can be formulated as a parametrized nonlinear operator equation in suitable Banach spaces. The frequency-dependent nondimensional parameter λ (the so-called Moiseyev detuning number λ) was treated as a *bifurcation parameter*, while $\tau > 0$ is a small *perturbation parameter* which characterizes an imperfection of the underlying system. The local bifurcation analysis of the operator problem gives results similar to those by Faltinsen *et al.*[8] However, a non-local analysis establishes a certain domain in the $(\lambda, \|\beta_1\|, \|\beta_2\|)$-space, where $\|\beta_2\| \sim \|\beta_1\|$ and, therefore, the relation (1.2) becomes invalid. Similar frequency domains were reported by Feng,[9,10] Faltinsen and Timokha[4,7] and, recently, by Wu.[34] In general, their existence is physically treated as the so-called internal (secondary) resonance.

Concepts of secondary resonances in the liquid sloshing dynamics have been elaborated by Ockendon *et al.*,[28,29] Bryant,[2] and Faltinsen and Timokha.[6] However, these works are concentrated on either shallow liquid depths or the case, when the forcing amplitude τ is not small. In both cases, higher modes are resonantly amplified, i.e. the modal functions β_i, $i \neq 1$, become of the same order as β_1. The analysis is then concentrated on excitations of the lowest natural mode, namely on the case when the forcing frequency σ is close to the lowest natural frequency σ_1.

However, the shallow liquid depth is characterized by the amplification of a large number of higher modes, i.e. $\beta_1 \sim \beta_i$, $i = 2, \ldots, N$, and N, generally speaking, tends to infinity. But the increase of τ with a finite liquid depth leads to the amplification of the second mode only, namely, $\beta_1 \sim \beta_2$. A similar amplification of higher modes β_3, β_4, etc. was only found slightly away from the primary resonance zone. It is a theoretical novelty that Part I establishes certain frequency domains in which $\|\beta_2\| \sim \|\beta_1\|$ for small τ and a finite liquid depths. These frequency domains do not vanish in the limit $\tau \to 0$.

There is a limited class of asymptotic modal systems that explain the amplification of higher modes due to the secondary resonance. Examples are given by Faltinsen and Timokha,[4,5] and Faltinsen *et al.*[7] However, the system by Faltinsen and Timokha[5] is based on the Boussinesq-type ordering and handles shallow liquid sloshing and Faltinsen *et al.*[7] operate with three-dimensional waves. Only the *adaptive* modal systems by Faltinsen and Timokha,[4] we believe, are applicable to study the steady-state solutions in the frequency domains established in Part I.

Based on a physical and experimental analysis, Faltinsen and Timokha[4] have proposed to consider the asymptotic relationships

$$\beta_i = O(\tau^{1/3}), \quad i = 1, \ldots, M; \quad \beta_i = O(\tau), \quad i > M, \tag{1.3}$$

where the number M may vary from 1 to ∞. By changing M, we obtain a series of *embedded* modal systems, which we call "Model M". Faltinsen and Timokha[4] studied the applicability of these models with increasing τ and in a wide range of the forcing frequency around the primary resonance. They found a good agreement between experimental data and theoretical results received with the Model 2 (based on the *double-dominant* relationship $\beta_1 \sim \beta_2 = O(\tau^{1/3})$, $\beta_i \leq O(\tau)$) in a local neighborhood of the primary resonance. This result was checked numerically by Landrini *et al.*[21] (smooth-particles hydromechanics method) and Löhner *et al.*[22] Model 3, Model 4 etc. are only needed for certain frequency domains away from the primary resonance zone.

The asymptotic modal system associated with Model 2 couples nonlinearly the two lowest (leading) modal functions. The remaining equations are linear in the driven modal functions β_i, $i \geq 3$, but may include nonlinear terms in β_1 and β_2. In the literature one finds no theoretical studies of this double-dominant system. Here, we use the operator approach of Part I to carry out a bifurcation analysis of its steady-state solutions and compare these results with those obtained with the single-dominant modal theory from Part I. We put the main emphasis on frequency domains, where $\beta_1 \sim \beta_2$, and on the critical depth-to-breadth ratio $h/l = 0.3368\ldots$.

2. Statement of the Problem and Preliminaries

2.1. *Definitions and nomenclature*

Having in mind the problem formulated in Part I, we consider two-dimensional oscillatory fluid flows in a rigid rectangular tank shaking horizontally with a frequency σ.

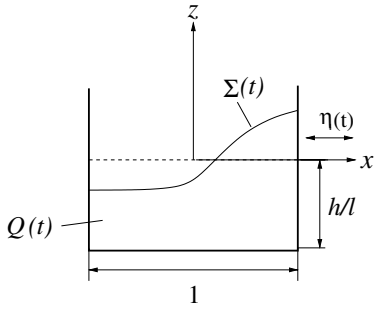

Fig. 1. Two-dimensional sloshing in a rectangular tank. Non-dimensional sketch, in which all the geometric sizes are scaled by the tank length l.

The amplitude of the shaking is small relative to the tank breadth l. An asymptotic analysis requires a nondimensional formulation, in which all the geometric parameters are scaled by l. Under this scaling, the time-dependent liquid volume reads (see Fig. 1):

$$Q(t) = \{(x, z) : -h < z < f(x, t); -1/2 < x < 1/2\}. \tag{2.1}$$

Let us define the hydrostatic liquid shape as $Q_0 = (-1/2, 1/2) \times (-h, 0)$ ($h := h/l$ is the scaled mean depth h) and $z = f(x, t)$ determines the free surface $\Sigma(t)$. The Oxz-coordinate system is fixed with the water-plane.

The original free boundary value problem (BVP) couples $f(x, t)$ and the velocity potential $\Phi(x, z, t)$ (see Part I of this work and the books of Moiseyev and Rumyantsev,[25] Lukovsky and Timokha,[23] and Ibrahim[17]). Adopting the multimodal methods, we have to introduce the Fourier solution of this free BVP

$$f(x, t) = \sum_{i=1}^{\infty} \beta_i(t) f_i(x); \quad \Phi(x, z, t) = -\tau x \sin t + \sum_{i=1}^{\infty} R_i(t) \phi_i(x, z), \tag{2.2}$$

where $f_i(x) = \cos(\pi i(x + 1/2))$ and

$$\phi_i(x, z) = f_i(x) \frac{\cosh(\pi i(z + h))}{\cosh(\pi i h)} \tag{2.3}$$

are the so-called natural modes. The natural sloshing frequencies (see, e.g. Faltinsen *et al.*[3,8]) are computed by

$$\sigma_i^2 = \frac{g}{l} \pi i \tanh(\pi i h), \quad i = 1, 2, \ldots, \tag{2.4}$$

where $g \approx 9.81\,\mathrm{m/s^2}$ is the gravitational acceleration.

Furthermore, in order to get a fully non-dimensional statement, we introduce the characteristic time $1/\sigma$ ($2\pi/\sigma$ is the forcing period) and re-define the time-coordinate as $t := \sigma t$. The nondimensional frequency parameter is then associated with the so-called Moiseyev detuning number (Moiseyev,[24] and Ockendon and

Ockendon[27])

$$\lambda = 1 - \frac{\sigma_1^2}{\sigma^2}, \quad -\infty < \lambda < 1. \tag{2.5}$$

Following Part I, λ is regarded as a *bifurcation parameter*.

Since the lateral harmonic excitation is performed with a small amplitude and one can define the non-dimensional forcing as

$$\eta_1 := \eta_1/l = \tau \cos t, \quad \tau \ll 1, \tag{2.6}$$

the problem contains an initial imperfection which is represented by the *perturbation parameter* τ. The parameter corresponds to the highest-order of smallness in the system.

2.2. *Modal systems*

2.2.1. *Single-dominant modal theory*

The single-dominant nonlinear modal theory by Faltinsen *et al.*[8] is based on the relations (1.2) and neglects $O(\delta^{4/3})$-terms. It results in a system of ODEs, whose first two equations are nonlinear in β_1 and β_2 and do not contain $\beta_i,\ i \geq 3$. The remaining equations are linear in $\beta_i,\ i \geq 3$, but may contain nonlinear terms in β_1 and β_2. If a 2π-periodic solution of the first two equations is found and substituted into the other modal equations, we can determine a numerical solution of $\beta_i(t),\ i \geq 3$, by standard techniques for linear differential equations with a periodic right-hand side. This means that the nonlinear intermodal energy content is completely determined by the two-dimensional subsystem for β_1 and β_2. This subsystem is the fundamental relation of the single-dominant modal theory and reads (see formulas (3.16) and (3.17) in Part I[16]) as

$$\begin{aligned} &\ddot{\beta}_1 + (1 - \delta_1(\lambda))\beta_1 + d_1(\ddot{\beta}_1\beta_2 + \dot{\beta}_1\dot{\beta}_2) + d_2(\ddot{\beta}_1\beta_1^2 + \dot{\beta}_1^2\beta_1) \\ &\qquad + d_3\ddot{\beta}_2\beta_1 + P_1\tau\cos t = 0; \end{aligned} \tag{2.7}$$

$$\ddot{\beta}_2 + (4 - \delta_2(\lambda))\beta_2 + d_4\ddot{\beta}_1\beta_1 + d_5\dot{\beta}_1^2 = 0. \tag{2.8}$$

Here,

$$\delta_i = \delta_i(\lambda) = i^2 - \mu_i^2(1 - \lambda); \quad \mu_i = \frac{\sigma_i}{\sigma_1},\ i \geq 1, \tag{2.9}$$

and the coefficients d_i, $i = 1, \ldots, 5$, and P_1 are defined by the formulas

$$\begin{aligned} &d_1 = 2\frac{E_0}{E_1} + E_1, \quad d_2 = 2E_0\left(-1 + \frac{4E_0}{E_1E_2}\right), \quad d_3 = -2\frac{E_0}{E_2} + E_1, \\ &d_4 = -4\frac{E_0}{E_1} + 2E_2, \quad d_5 = E_2 - 2\frac{E_0E_2}{E_1^2} - \frac{4E_0}{E_1}, \quad P_1 = \frac{4\tanh(\pi h)}{\pi}, \end{aligned} \tag{2.10}$$

where

$$E_0 = \frac{\pi^2}{8}, \quad E_i = \frac{\pi}{2}\tanh(\pi i h), \quad i \geq 1. \tag{2.11}$$

2.2.2. *Double-dominant modal theory*

Having in mind an amplification of the second modal function β_2 for certain values of λ and increasing τ, Faltinsen and Timokha[4] proposed an adaptive modal theory. As Model 2 of this theory, they derived an asymptotic modal system based on

$$\beta_1 \sim \beta_2 \sim \delta^{1/3}, \quad \beta_i \sim \delta, \;\; i \geq 3. \tag{2.12}$$

Similarly to the single-dominant case, the basis of this new theory consists of the two nonlinear second-order ODEs for the unknown functions $\beta_1(t)$ and $\beta_2(t)$:

$$\ddot{\beta}_1 + (1-\delta_1(\lambda))\beta_1 + d_1(\ddot{\beta}_1\beta_2 + \dot{\beta}_1\dot{\beta}_2) + d_2(\ddot{\beta}_1\beta_1^2 + \dot{\beta}_1^2\beta_1) + d_3\ddot{\beta}_2\beta_1 + \tilde{d}_1\ddot{\beta}_1\beta_2^2 + \tilde{d}_2\ddot{\beta}_2\beta_2\beta_1 + \tilde{d}_3\dot{\beta}_2^2\beta_1 + \tilde{d}_4\dot{\beta}_1\dot{\beta}_2\beta_2 + P_1\tau\cos t = 0; \tag{2.13}$$

$$\ddot{\beta}_2 + (4-\delta_2(\lambda))\beta_2 + d_4\ddot{\beta}_1\beta_1 + d_5\dot{\beta}_1^2 + \tilde{d}_5\ddot{\beta}_1\beta_1\beta_2 + \tilde{d}_6\ddot{\beta}_2\beta_1^2 + \tilde{d}_7(\ddot{\beta}_2\beta_2^2 + \dot{\beta}_2^2\beta_2) + \tilde{d}_8\dot{\beta}_1^2\beta_2 + \tilde{d}_9\dot{\beta}_1\dot{\beta}_2\beta_1 = 0. \tag{2.14}$$

The remaining differential equations are rather complicated, but they are still linear in β_i, $i \geq 3$.

Equations (2.7) and (2.8) contain additional (relative to (2.13), (2.14)) nonlinear terms associated with nine coefficients $\tilde{d}_i$, $i = 1, \ldots, 9$. Using the tensor expressions from Faltinsen and Timokha,[4] these coefficients can be written in the following form

$$\tilde{d}_1 = -4E_0 + 4\frac{E_0^2}{E_1^2} + 12\frac{E_0^2}{E_1E_3}; \quad \tilde{d}_2 = -4\frac{E_0^2}{E_1E_2} + 12\frac{E_0^2}{E_2E_3},$$

$$\tilde{d}_3 = 8\frac{E_0E_1}{E_2} - 4\frac{E_0^2}{E_1E_2} + 12\frac{E_0^2}{E_2E_3} - 4\frac{E_0^2}{E_2^2} - 12\frac{E_0^2E_1}{E_2^2E_3},$$

$$\tilde{d}_4 = -8E_0 + 8\frac{E_0^2}{E_1^2} + 24\frac{E_0^2}{E_1E_3}; \quad \tilde{d}_5 = -8\frac{E_0^2}{E_1^2} + 24\frac{E_0^2}{E_1E_3},$$

$$\tilde{d}_6 = -16E_0 + 8\frac{E_0^2}{E_1E_2} + 24\frac{E_0^2}{E_2E_3}; \quad \tilde{d}_7 = -8E_0 + 32\frac{E_0^2}{E_2E_4},$$

$$\tilde{d}_8 = 8\frac{E_0E_2}{E_1} - 8\frac{E_0^2}{E_1^2} + 24\frac{E_0^2}{E_1E_3} - 8\frac{E_0^2E_2}{E_1^3} - 24\frac{E_0^2E_2}{E_1^2E_3},$$

$$\tilde{d}_9 = -32E_0 + 16\frac{E_0^2}{E_1E_2} + 48\frac{E_0^2}{E_2E_3}.$$

The postulation of (2.12) was based on a physical and experimental analysis. Faltinsen and Timokha[4] have shown that numerical simulations on the basis of (2.13), (2.14) are in a good agreement with experimental data for $h \geq 0.24$ and $\tau \leq 0.1$. The range for the frequency parameter λ should be $\lambda_0(2,2) < \lambda < 1$ (see, Part I and Fig. 2), where $\lambda = 0$ means primary resonance (as follows from the definition (2.5)). A failure of this model was only found when an increase of the forcing causes a fragmentation of the free surface in experimental observations.

Simulations and experimental data by Faltinsen and Timokha[4] have shown that an explanation for the amplification of the third mode, i.e. $\beta_1 \sim \beta_2 \sim \beta_3$, is required. The consequence is the development of a new modal system of dimension 3, Model 3, which is only appropriate when λ is away from the mentioned frequency range, namely, $\lambda < \lambda_0(2,2)$.

2.3. *Operator statement and preliminary results*

2.3.1. *Operator formulation*

In order to get an operator formulation of the single-dominant system equipped by periodic boundary conditions, in Part I, we have set $B = (\beta_1, \beta_2)^{\mathrm{T}}$ and rewritten the nonlinear equations (2.7) and (2.8) as

$$M(B)\ddot{B} = G^M(t, B, \dot{B}; \lambda, \tau), \tag{2.15}$$

with

$$M = \begin{pmatrix} 1 + d_1\beta_2 + d_2\beta_1^2 & d_3\beta_1 \\ d_4\beta_1 & 1 \end{pmatrix} \in \mathbb{R}^{2\times 2} \quad \text{and} \quad G^M = (G_1^M, G_2^M) \in \mathbb{R}^2,$$

$$\begin{aligned} G_1^M &= -(1-\lambda)\beta_1 - d_1\dot{\beta}_1\dot{\beta}_2 - d_2\dot{\beta}_1^2\beta_1 - P_1\tau\cos t, \\ G_2^M &= -(4-\delta_2(\lambda))\beta_2 - d_5\dot{\beta}_1^2. \end{aligned} \tag{2.16}$$

Similarly, Eqs. (2.13) and (2.14) can be written in the form (2.15) with

$$M = \begin{pmatrix} 1 + d_1\beta_2 + d_2\beta_1^2 + \tilde{d}_1\beta_2^2 & d_3\beta_1 + \tilde{d}_2\beta_1\beta_2 \\ d_4\beta_1 + \tilde{d}_5\beta_1\beta_2 & 1 + \tilde{d}_6\beta_1^2 + \tilde{d}_7\beta_2^2 \end{pmatrix} \in \mathbb{R}^{2\times 2} \tag{2.17}$$

and

$$\begin{aligned} G_1^M &= -(1-\lambda)\beta_1 - d_1\dot{\beta}_1\dot{\beta}_2 - d_2\dot{\beta}_1^2\beta_1 - \tilde{d}_3\dot{\beta}_2^2\beta_1 - \tilde{d}_4\dot{\beta}_1\dot{\beta}_2\beta_2 - P_1\tau\cos t, \\ G_2^M &= -(4-\delta_2(\lambda))\beta_2 - d_5\dot{\beta}_1^2 - \tilde{d}_8\dot{\beta}_1^2\beta_2 - \tilde{d}_7\dot{\beta}_2^2\beta_2 - \tilde{d}_9\dot{\beta}_1\dot{\beta}_2\beta_1. \end{aligned} \tag{2.18}$$

As long as B is relatively small in a uniform norm, the matrix M is nonsingular and, therefore, one can use the normal form

$$\ddot{B} = G(t, B, \dot{B}; \lambda, \tau), \tag{2.19}$$

where $G = M^{-1}G^M$ and $G : D_G := [0, 2\pi] \times D_B \times D_{\dot{B}} \times \mathbb{R} \times \mathbb{R} \to \mathbb{R}^2$, $0 \in D_G$, $G \in C^p(D_f)$, $p \geq 4$.

Furthermore, we assume that Eq. (2.19) is subject to the periodic boundary conditions

$$l_0(B) = B(0+) - B(2\pi-) = 0, \quad l_1(\dot{B}) = \dot{B}(0+) - \dot{B}(2\pi-) = 0, \tag{2.20}$$

and consider the parametrized nonlinear BVP (2.19), (2.20) as an operator equation

$$T(B; \lambda; \tau) := \ddot{B} - G(t, B, \dot{B}; \lambda, \tau) = 0, \quad B \in X, \quad \lambda, \tau \in \mathbb{R}. \tag{2.21}$$

Here, $T : Z := X \times \mathbb{R} \times \mathbb{R} \to Y$ and the Banach spaces X, Y

$$X := BC^2([0, 2\pi], \mathbb{R}^2) := \{B \in C^2([0, 2\pi], \mathbb{R}^2) : l_0(B) = 0, l_1(\dot{B}) = 0\},$$

$$Y := C([0, 2\pi], \mathbb{R}^2)$$

are equipped by the norms

$$\|B\|_X = \|B : BC^2\| = \|B : C^2\| = \sup_{t\in[0,2\pi]} (|B(t)| + |\dot{B}(t)| + |\ddot{B}(t)|),$$

$$\|B\|_Y = \|B : C\| = \sup_{t\in[0,2\pi]} |B(t)|.$$

The operator equation (2.21) depends on two real parameters $-\infty < \lambda < 1$ and $0 \le \tau \ll 1$. Let us assume that τ belongs to an interval I_τ. Following Hermann,[13] Wallisch and Hermann,[32] and Hermann and Ullrich,[15] we study the solution manifold

$$\mathcal{M} := \{(B, \lambda, \tau) : -\infty < \lambda < 1;\ \tau \in I_\tau;\ T(B, \lambda, \tau) = 0\}. \tag{2.22}$$

Obviously, the trivial solution curve $C_{\text{triv}} := \{(0, \lambda, 0) : -\infty < \lambda < 1\}$ belongs to $\mathcal{M}$ and can be interpreted as the hydrostatic equilibrium of the original sloshing problem.

2.3.2. *Primary bifurcation points on the trivial solution curve* C_{triv}

A local analysis of the manifold $\mathcal{M}$ should include the detection of the primary bifurcation points on C_{triv}. These appear at certain values $\{\lambda_0(i, k)\}$, the so-called *critical values*, on the abscissa of the $(\lambda, \|B\|)$-plane, at which non-trivial solutions of (2.21) are branching off. From a physical point of view, the existence of these bifurcation points implies nonlinear free-standing waves.

In order to find $\{\lambda_0(i, k)\}$, let us present the unperturbed problem (2.21) (i.e. the case $\tau = 0$) as

$$T(B; \lambda, 0) = T_0(B; \lambda) := T_B^0[\lambda]B + \tilde{T}_0(B; \lambda) = 0, \quad T_0 : X \times \mathbb{R} \to Y, \tag{2.23}$$

where $T_B^0[\lambda]B$ is the linear part of the operator T_0 which is represented by the Fréchet derivative $T_B^0[\lambda] = \partial T_0(0, 0)/\partial B$. It can easily be shown that $T_B^0[\lambda]$ is a self-adjoint Fredholm operator on a suitable set of functions from $L_2(0, 2\pi)$. The linearised problem

$$T_B^0[\lambda]\varphi = 0, \quad \varphi \in X, \tag{2.24}$$

has the eigenvalues

$$\lambda_0(i, k) = 1 - k^2/\mu_i^2, \quad k \in \mathbb{N},\ \ i = 1, 2, \tag{2.25}$$

which are the required critical values of (2.23). Note, that we have determined the same values of $\lambda_0(i, k)$ in Part I. The reason is that the linearizations of (2.7)–(2.8) and (2.13)–(2.14) are identical.

Since $\mu_1^2 = 1$ and $2 < \mu_2^2 < 4$, there do not exist two integers k_1 and k_2 such that $\lambda_0(1, k_1) = \lambda_0(2, k_2)$. This implies that the two kernels $\mathcal{N}(T_B^0[\lambda_0(i, k)])$,

$i = 1, 2$, have dimension 2 and are spanned by either $\varphi_1[1,k] = (\sin(kt), 0)$ and $\varphi_2[1,k] = (\cos(kt), 0)$ or $\varphi_1[2,k] = (0, \cos(kt))$ and $\varphi_2[2,k] = (0, \sin(kt))$. Moreover, the kernels $\mathcal{N}(T_B^0[\lambda_0(i,k)]^*)$ of the adjoint operators $T_B^0[\lambda_0(i,k)]^*$, $i = 1, 2$, have dimension two as well and are spanned by $\psi_m[i,k] = \varphi_m[i,k]$, $m, i = 1, 2$; $k \in \mathbb{N}$. This dimension is caused by the phase-shift invariance, i.e. the kernels have the following structure

$$\mathcal{N}(T_B^0[\lambda_0(i,k)]) = \begin{cases} c \cdot (\cos(k(t+\theta)), 0), & \text{for } i = 1, \\ c \cdot (0, \cos(k(t+\theta))), & \text{for } i = 2, \end{cases}$$

where $\theta \in \mathbb{R}$ can be fixed without loss of generality.

The values $\lambda_0(i,k)$, $i = 1, 2$, $k \geq 1$, change with the mean fluid depth h. In general, their order along the λ-axis is not clearly predictable. However, one can show that the three lowest critical values satisfy: $\lambda(1,1) = 0$, $\lambda(2,2) \in (-1, 0)$ and $\lambda(2,1) \in (1/2, 3/4)$. Moreover, it holds $\lambda_0(2,2) < \lambda < \lambda_0(2,1)$ and $\lambda(2,2) \to 0$ as $h \to 0$.

2.3.3. *Applicability of the single-dominant modal theory*

In the previous section we have demonstrated that the unperturbed operator problem has an infinite number of primary bifurcation points at $\lambda_0(i,k) \in \mathbb{R}$, $i = 1, 2$, $k = 1, 2, \ldots$, on the λ-axis. The theory presented in Part I has proved that these primary bifurcations are destroyed by imperfections $\tau > 0$ only at two values, namely at $\lambda_0(1,1) = 0$ (the local branching behavior is consistent with Moiseyev[24] and Faltinsen[3]) and at $\lambda_0(2,2)$. The primary bifurcations are preserved at the other points.

From a physical point of view, the first bifurcation point ($\lambda = \lambda_0(1,1) = 0$) implies primary resonance. When $\lambda \to \lambda_0(2,2) \neq 0$, the forcing frequency is away from the primary resonance zone. The destroyed primary bifurcation at $\lambda_0(2,2)$ means a secondary (internal) resonance. A concept of this type of secondary resonance was elaborated in the physical literature (Feng,[9,10] Ockendon *et al.*,[28,29] Bryant,[2] and Faltinsen and Timokha[4,5]). A simple treatment of this concept is that, for a certain value of $\lambda \approx \lambda_0(2,2)$, the second-order quantities in Eqs. (2.8)–(2.14) generate a double-frequency harmonics $\cos 2t$ and $\sin 2t$ and this double harmonics may be close to the second natural sloshing frequency, i.e. under our non-dimensional statement, close to $\sqrt{4 - \delta_2(\lambda)}$. Occurrence of the secondary resonance at $\lambda_0(2,2)$ leads to an increase of $\|\beta_2\|$. It reaches the order of magnitude of $\|\beta_1\|$ or even exceeds this value. As a consequence, the asymptotic relation (1.2) fails. In Part I the branching at $\lambda_0(2,2)$ is analyzed with the single-dominant theory.

Another discovery of Part I is a frequency domain in the vicinity of $\lambda(1,1) = 0$ where the nonlocal solution of (2.21) is characterized by the relation $\beta_2 \sim \beta_1$. The domain does not vanish as τ decreases and, we believe, a new type of secondary resonance is indicated. It occurs away from $\lambda_0(2,2)$ and for small values of τ. This frequency domain will be the primary focus of our study in Sec. 5.

3. Unperturbed Operator Problem for the Double-Dominant Theory

The results of the Lyapunov–Schmidt reduction in a neighborhood of $\lambda_0(1,k)$, $k \in \mathbb{N}$, coincide with those presented in Part I for (2.7) and (2.8), i.e. the local branching can be described as

$$\begin{aligned} \beta_1(t;s) &= s\cos(k(t+\theta)) + O(s^3);\\ \beta_2(t;s) &= s^2[p_0 + h_0\cos(2k(t+\theta))] + O(s^4);\\ \lambda(s) &= 1 - k^2 + s^2k^2m_1 + O(s^4), \end{aligned} \tag{3.1}$$

where $|s| \le s_0 \ll 1$ is an artificial parameter,

$$p_0 = \frac{d_4 - d_5}{2\mu_2^2}, \quad h_0 = \frac{d_4 + d_5}{2(\mu_2^2 - 4)} \tag{3.2}$$

and

$$m_1 = -\frac{1}{2}d_2 - d_1\left(p_0 - \frac{1}{2}h_0\right) - 2h_0d_3 \tag{3.3}$$

depends only on the mean fluid depth h.

The local solutions bifurcating at $\lambda_0(2,k)$, $k \in \mathbb{N}$, differ from the results given in Part I and now take the form

$$\begin{aligned} &\beta_1(t;s) \equiv 0; \quad \beta_2(t;s) = s\cos(k(t+\theta)) + O(s^3),\\ &\lambda(s) = 1 - \frac{k^2}{\mu_2^2} - s^2\frac{\tilde{d}_7k^2}{2\mu_2^2} + O(s^3), \quad |s| \le s_0 \ll 1. \end{aligned} \tag{3.4}$$

The parametrized solutions (3.1) and (3.4) determine the local branching at the primary bifurcation points. Considering the situation in the $(\lambda, \|\beta_1\|, \|\beta_2\|)$-space, we find that the curves associated with (3.4), which emerge at $\lambda_0(2,k)$, $k \ge 1$, run in the $(\lambda, \|\beta_2\|)$-plane. In contrast, the representation (3.1) determines almost planar branches in the $(\lambda, \|\beta_1\|)$-plane. Curves bifurcating at the lower critical values $\lambda_0(i,k)$ are exemplified in Fig. 2.

The type of the local branching (soft- or hard-spring behavior) depends on the signs of m_1 and $\tilde{d}_7$. A simple analysis shows that $\tilde{d}_7 > 0$ for arbitrary h. This means that the solutions on the curves emerging at $\lambda_0(2,k)$, $k \ge 1$, are characterized by the *soft-spring* behavior. The corresponding examples for $\lambda_0(2,k)$, $k = 1,2,3$, are plotted in Fig. 2 (solid lines). Dashed lines represent the primary bifurcating solution curves which are determined by the single-dominant theory.

The qualitative conclusions on the branching behavior at the critical values $\lambda_0(1,k)$, $k = 1,2,3$, are the same as presented in Part I. In Fig. 2, the curves branching off at $\lambda_0(1,1) = 0$ and $\lambda_0(1,2) = -3$ are represented by solid lines. When $m_1 < 0$ ($h > h_R = 0.3368\ldots$), the corresponding solutions determine the *soft-spring* behavior, but $m_1 > 0$ ($h < h_R$) is associated with the *hard-spring* behavior.

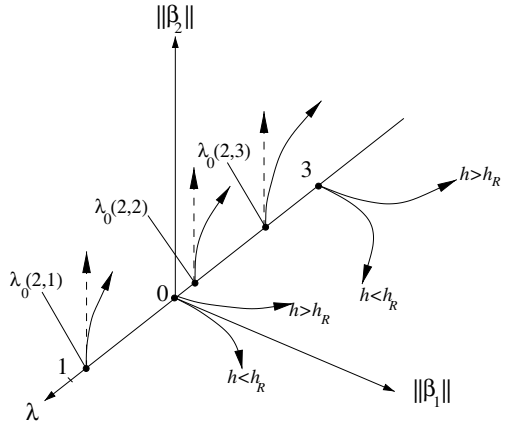

Fig. 2. Local branching at $\lambda_0(i,k)$, $i=1,2$, $k\in\mathbb{N}$, in the $(\lambda,\|\beta_1\|,\|\beta_2\|)$-space. The solid lines: curves branching off at $\lambda_0(1,1)=0$ and $\lambda_0(1,2)=-3$ in the $(\lambda,\|\beta_1\|)$-plane; curves branching off at $\lambda_0(2,k)$, $k=1,2,3$, in the $(\lambda,\|\beta_2\|)$-plane. The dashed vertical lines: curves branching off at $\lambda_0(2,k)$, $k=1,2,3$, which have been computed in Part I using the single-dominant model (2.7), (2.8). The behavior at $\lambda_0(1,k)=1-k^2$, $k\in\mathbb{N}$, depends on h: $h>h_R=0.3368\ldots$ leads to the *soft-spring* behavior, but $h<h_R$ implies the *hard-spring* behavior.

4. Local Analysis of the Perturbed Bifurcations

When $\tau>0$, the perturbed operator equation (2.21) describes the forced steady-state waves. The smallness of τ makes it possible to use the Lyapunov–Schmidt reduction and to analyze perturbations of the branching solutions in a neighborhood of $\lambda_0(i,k)$, $i=1,2$, $k\in\mathbb{N}$. The procedure employs the fact that $\dim\mathcal{N}(T_B^0[\lambda_0(i,k)])=2$ and is in some detail described in Part I. The analysis suggests $\tau\ll|s|$, where s is the artificial parameter in the ansatz (3.1) and (3.4), respectively, for the local solutions. The Lyapunov–Schmidt reduction shows that the initial perturbations τ can either *preserve* or *destroy* the primary (unperturbed) bifurcation points.

4.1. *Perturbed bifurcations at* $\lambda_0(1,k)$, $k\in\mathbb{N}$

The analysis of the perturbed bifurcations at $\lambda_0(1,k)$, $k\in\mathbb{N}$, leads to the same results as those presented in Part I of this work. For $k\neq1$, the initial perturbations τ *preserve* the bifurcating solutions (3.1). In that case, any small $\tau\ll s$ does not effect the dominating asymptotic terms in (3.1). Therefore, the branching solutions can be parametrized in the form

$$\begin{aligned}\beta_1(t;s)&=s\cos(k(t+\theta))-\frac{P_1\tau}{k^2-1}\cos t+O(s^3);\\ \beta_2(t;s)&=s^2[p_0+h_0\cos(2k(t+\theta))]+O(s\tau);\\ \lambda(s)&=1-k^2+s^2k^2m_1+O(s\tau),\quad |s|\le s_0\ll1,\end{aligned}\tag{4.1}$$

where m_1 is determined by (3.3).

In contrast, for $k = 1$, the perturbations τ *destroy* the local bifurcating solutions (3.1). The local solutions can now be represented in the form

$$\begin{gathered}\beta_1(t;s) = s\cos(t) + O(s^2); \quad \beta_2(t;s) = s^2(p_0 + h_0\cos 2t) + O(s^3),\\ \lambda(s) = \left(m_1 + \frac{P_1\tau}{s^3}\right)s^2 + O(s^3), \quad |s| \le s_0 \ll 1.\end{gathered} \tag{4.2}$$

The representation (4.2) is based on the relation $s^3 \sim \tau$ which is in fact a resolvability condition.

4.2. *Perturbed bifurcations at* $\boldsymbol{\lambda_0(2,k)}$, $\boldsymbol{k \in \mathbb{N}}$

The results on the perturbed bifurcations at $\lambda_0(2,k)$, $k \in \mathbb{N}$, differ from those given in Part I. Here, the initial perturbations τ can either *preserve* ($k \neq 2$, $k \in \mathbb{N}$) or *destroy* ($k = 2$) the unperturbed bifurcations associated with the local solutions (3.4). If $k \neq 2$, the Lyapunov–Schmidt reduction gives

$$\begin{gathered}\beta_1(t;s) = s_k\tau\cos t + O(\tau s); \quad \beta_2(t;s) = s\cos(k(t+\theta)) + O(s^3),\\ \lambda(s) = 1 - \frac{k^2}{\mu_2^2} - s^2\frac{\tilde{d}_7k^2}{2\mu_2^2} + O(s^3), \quad |s| \le s_0 \ll 1,\end{gathered} \tag{4.3}$$

where $s_k = -P_1/(k^2/\mu_2^2 - 1) = O(1)$.

In the case $k = 2$, the situation changes. Now, the initial perturbations τ *destroy* the bifurcations appearing in the unperturbed problem and generate the following local solution

$$\begin{gathered}\beta_1(t;s) = s_2\tau\cos t + O(\tau s); \quad \beta_2(t;s) = s\cos 2t + O(s^3),\\ \lambda(s) = 1 - \frac{4}{\mu_2^2} - \left(\frac{2\tilde{d}_7}{\mu_2^2} + \frac{s_2^2(d_4+d_5)}{2\mu_2^2}\cdot\frac{\tau^2}{s^3}\right) + O(s^3), \quad |s| \le s_0 \ll 1,\end{gathered} \tag{4.4}$$

where the resolvability condition now reads $\tau^2 \sim s^3$.

4.3. *Local response curves*

The bifurcation preserving perturbations, associated with the solutions (4.1) and (4.3), do not introduce a new resolvability condition. Since the s-dependent terms in these solutions are independent of τ, the problem can be related to the free nonlinear sloshing. From a physical point of view, the sloshing is characterized by a small viscous damping. This leads to a rapid decaying of this free nonlinear sloshing. Moreover, the solutions (4.1) and (4.3) without the s-terms describe in fact a linear sloshing.

In contrast to the bifurcation preserving perturbations, the relations (4.2) and (4.4) couple τ and s. Varying $\lambda \in (-\infty, 1)$ and choosing appropriate values of s (independently of τ), determines a local branching structure for a relatively small norm $\|B\|$. In Fig. 3(a), (b), this branching is shown in the $(\lambda, \|B\|)$-plane for $h > h_R$

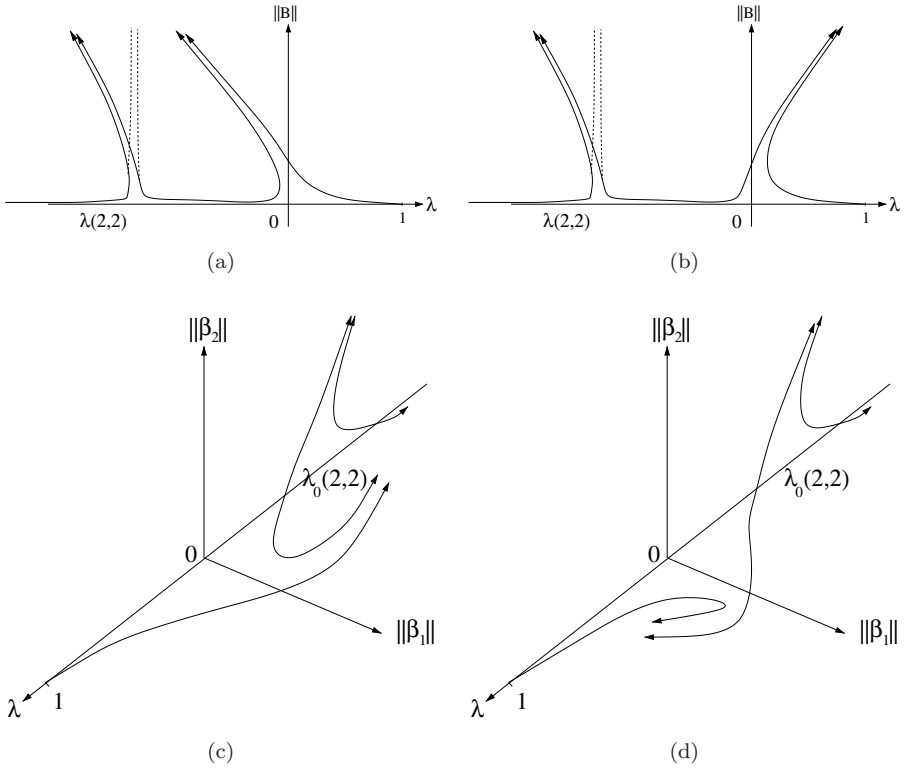

Fig. 3. Perturbed local bifurcations associated with the solutions (4.1)–(4.4). The representations are given in the $(\lambda, \|B\|)$-plane (see, (a) and (b)) and in the $(\lambda, \|\beta_1\|, \|\beta_2\|)$-space (see, (c) and (d)). The solid lines: cases (a), (c) imply $h > h_R$, but (b) and (d) correspond to $h < h_R$. The dashed lines: the local behavior at $\lambda_0(2,2)$ for the single-dominant system (2.7), (2.8) is illustrated in (a) and (b).

and $h < h_R$, respectively. Here the curves at the origin are associated with the local solution (4.2) (for $\lambda \to \lambda_0(1,1) = 0$). The behavior of $\|B\|$ as $\lambda \to \lambda_0(2,2)$ is described by the solution (4.4).

As mentioned above, the local solution (4.2) implies the local branching at the bifurcation point $\lambda_0(1,1)$. This point is related to the primary resonance in the system when $\sigma \to \sigma_1$. This type of resonance was described by Faltinsen.[3] Thus, it is evident that the solution (4.2) is mathematically equivalent to his results. Although Ockendon *et al.*,[28,29] Faltinsen and Timokha[4,6] and other authors clarified why we should expect a secondary resonance at point $\lambda_0(2,2)$, the analysis of the corresponding local nonlinear amplification of the second mode at $\lambda_0(2,2)$ is, to the authors knowledge, absent in the literature. This means that the local solution (4.4) is a pioneering one. When nonlinearity associated with $\tilde{d}_7$ is neglected, the branching at $\lambda_0(2,2)$ has a *linear* character as it has been in the case of the single-dominant theory. This fact becomes clear when the dashed and solid lines in Fig. 3(a), (b) are compared.

Finally, our primary attention should be on the frequency domains at $\lambda \approx 0$, where in Part I an amplification of the second mode has been detected, i.e. $\beta_2 \sim \beta_1$. This happens due to fact that the branching at this point may become strongly three-dimensional in the $(\lambda, |\beta_1|, |\beta_2|)$-space as it is schematically shown in Fig. 3(c), (d). When m_1 is finite, this domain is slightly away from the λ-axis. As long as m_1 tends to zero, namely, $h \to 0.3368\ldots$, the frequency domain touches this axis. This behavior requires a special study of the local and nonlocal branching for the critical depth.

5. Non-Local Branching

The nonlocal behavior of the perturbed response curves ($\tau > 0$) is studied by using the RWPM-package of Hermann and Kaiser,[14] and Hermann and Ullrich.[15] We focus on what happens in a neighborhood of $\lambda = \lambda_0(1,1) = 0$, where in Part I a new type of secondary resonance is established. Moreover, the linear (single-dominant) and nonlinear (double-dominant) branches at $\lambda_0(2,2)$ are compared.

A typical nonlocal branching for three different fluid depths is illustrated in the Figs. 4–6. Each figure consists of three parts. These parts represent the three-dimensional response curves in the $(\lambda, \|\beta_1\|, \|\beta_2\|)$-space and their projections on the $(\lambda, \|\beta_1\|)$- and $(\lambda, \|\beta_2\|)$-planes. The solid lines are used to mark the results obtained with the double-dominant modal theory and the dashed lines give the branching obtained with the single-dominant theory. Our calculations were made for $\tau = 0.01$. This value of the perturbation parameter (non-dimensional forcing amplitude) is relevant to various laboratory experiments in which τ typically varies from 0.005 to 0.05. Furthermore, the limit of the branching for $\tau \to 0$ is presented by dashed-and-dotted (double-dominant) and dotted (single-dominant) curves in parts (a) of Figs. 4–6. These represent the nonlocal branching of the unperturbed problem. A splitting of the curves implies that the single-dominant theory fails in the asymptotic limit $\tau \to 0$. In Figs. 4 and 6, the splitting occurs in a domain of the $(\lambda, \|\beta_1\|)$-plane which is far from the λ-axis. However, in Fig. 5 the splitting occurs at the origin which can be attributed to the critical depth. When τ is a small fixed positive number, e.g. $\tau = 0.01$ as in Figs. 4–6, the disagreement between the two theories can clearly be seen at the two resonant zones. The disagreement is especially evident for the critical depth case.

Figure 4 shows the response curves for $h = 0.5$, i.e. for the case when the local analysis predicts a *soft-spring* local branching at $\lambda = 0$. Parts (a) and (b) demonstrate that the nonlocal branching determined by the double-dominant theory keeps this local behavior even when the norm of B increases. But this is not true for the single-dominant theory. We illustrate this fact in part (a), where the secondary bifurcation point S on the *backbone* (dotted line, unperturbed operator problem for the single-dominant theory) is discovered. Furthermore, a comparison of parts (a) and (b) shows that the relation $\beta_1 \sim \beta_2$ can be fulfilled for the nonlocal branches

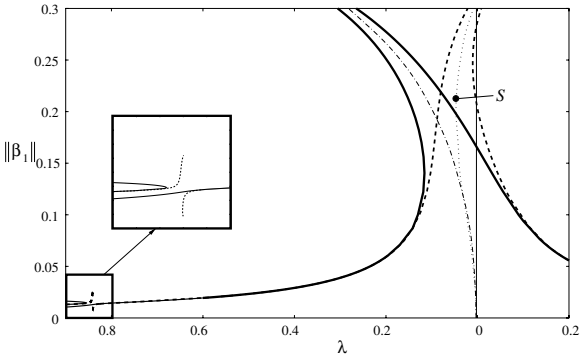

(a)

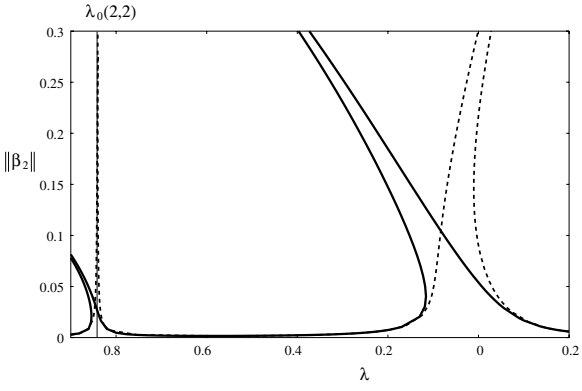

(b)

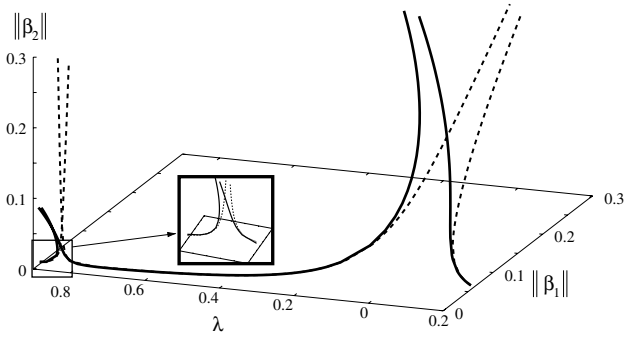

(c)

Fig. 4. Typical response curves for $h > h_R$, i.e. for the case when the local bifurcation analysis predicts the *soft-spring* behavior at $\lambda = \lambda_0(1,1) = 0$. Computations were done with $h = 0.5$, $\tau = 0.01$. Solid lines: results obtained by using the double-dominant modal theory. Dashed lines: results obtained by the single-dominant theory. The figure consists of three parts: (a) the response curves in the $(\lambda, \|\beta_1\|)$-plane; (b) the response curves in the $(\lambda, \|\beta_2\|)$-plane, and (c) the three-dimensional $(\lambda, \|\beta_1\|, \|\beta_2\|)$-view. The dotted line in (a) depicts the response curve for the unperturbed problem ($\tau = 0$) which has been determined with the single-dominant theory. The dashed-and-dotted line denotes the unperturbed response curve determined by the double-dominant theory.

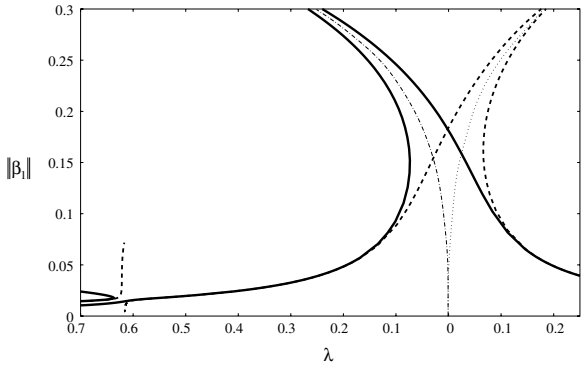

(a)

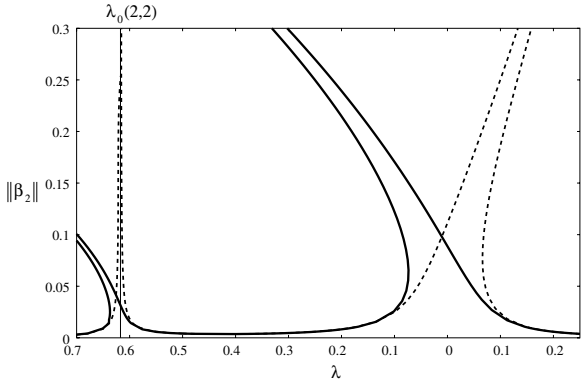

(b)

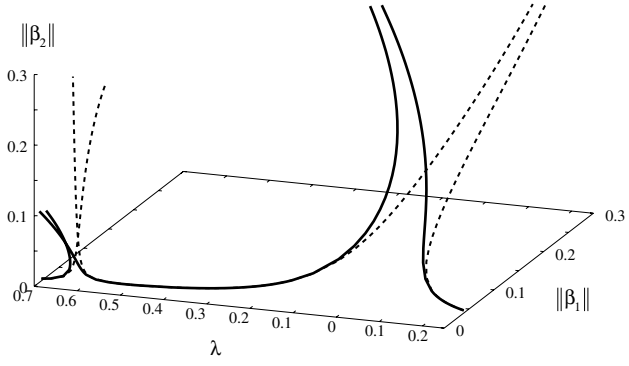

(c)

Fig. 5. The same as in Fig. 4, but for the value $h = h_R = 0.3368\ldots$.

at both $\lambda = 0$ and $\lambda = \lambda_0(2,2)$. This implies that the single-dominant theory based on the asymptotics (1.2) fails with increasing $\|B\|$ and, therefore, the secondary bifurcation point S is physically irrelevant. In contrast, the relation $\|\beta_1\| \sim \|\beta_2\|$ is consistent with the original assumption (2.12).

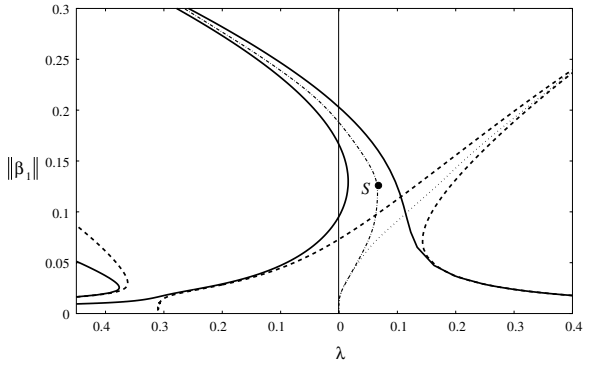

(a)

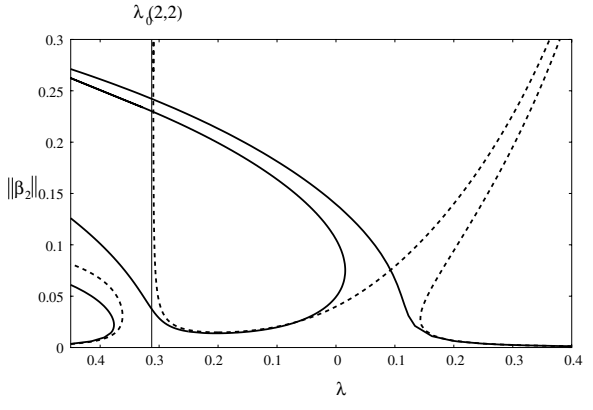

(b)

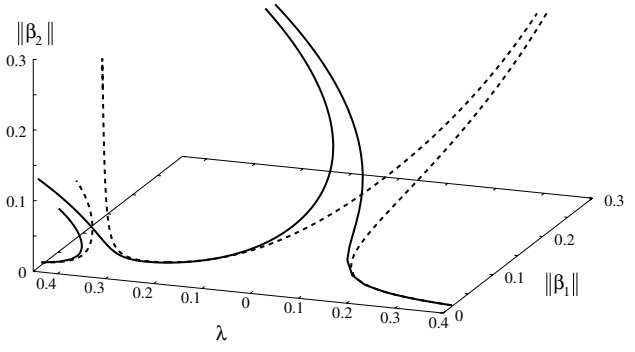

(c)

Fig. 6. The same as in Fig. 4, but for the case when the local branching at $\lambda = 0$ is characterized by the *hard-spring* behavior. The calculations were done for the value $h = 0.2$.

Figure 5 demonstrates a nonlocal branching for $h = h_R = 0.3368\ldots$, i.e. when the local analysis predicts a change from *soft-spring* to *hard-spring* behavior at $\lambda = 0$. The calculations show two qualitatively different results for the single- and double-dominant modal systems. The branches for the single-dominant case indicate

a *hard spring*-like behavior, whereas the double-dominant theory clearly establishes *soft spring*-like branching. We indicate it by dotted and dashed-and-dotted lines in part (a). In order to find out which parts of these branches are physically relevant, one should compare the norms $\|\beta_2\|$ and $\|\beta_1\|$ in parts (a) and (b). It follows that $\|\beta_1\| \sim \|\beta_2\|$ as $\lambda \to 0$. Therefore, from a physically point of view, we can only trust the results obtained with the double-dominant theory. The *soft spring*-like perturbed branching for the theoretical $h = h_R = 0.3368\ldots$ is consistent with the famous laboratory tests by Fultz,[12] who estimated the experimental critical depth at $h = 0.28$. *Soft spring*-like nonlocal branching for $h = h_R$ was also deduced by a special fifth-order sloshing theory of Waterhouse.[33]

Figure 6 illustrates the response curves for $h < h_R$, when the *hard-spring* unperturbed local branching at $\lambda = 0$ is expected. In the calculations we used $h = 0.2$. This is the lower bound for the applicability of the double-dominant theory. Smaller h belongs to the so-called intermediate, or shallow liquid depth ranges. The most interesting conclusion which follows from a comparison of parts (a) and (b) of this figure, is that the double-dominant theory is characterized by a secondary bifurcation in the unperturbed problem (point S on the dashed-and-dotted line). Another important fact is that the nonlocal results obtained by the single-dominant theory (dashed lines) at $\lambda = 0$ clearly contradict the intermodal ordering (1.2) for the tested value of τ, whereas the double-dominant theory is consistent with the assumption $\beta_1 \sim \beta_2$. We illustrate also a dramatical increase of the norm $\|\beta_2\|$ for $\lambda \approx \lambda_0(2,2)$ (compare the solid lines around $\lambda = \lambda_0(2,2)$ in parts (a) and (b) of Fig. 6 as well as in parts (b) of Figs. 4–6). From a physical point of view, this may indicate the amplification of some higher modes, e.g. $\beta_1 \sim \beta_2 \sim \beta_3$, due to energy content from β_1 and β_2. Physical aspects of those amplifications as $h \to 0$ with a fixed τ were extensively discussed by Faltinsen and Timokha.[5] In this case, the modeling at $\lambda_0(2,2)$ may require another modal system from our Model 2, e.g. Model 3 by Faltinsen and Timokha,[4] or the Boussinesq-like model by Faltinsen and Timokha.[5] We will discuss this point in Sec. 7.

6. On the Experimental Critical Depth

As we have shown above, the single-dominant theory fails at the primary resonant point $\lambda = 0$ for h close to the theoretical value $h_R = 0.3368\ldots$. A successful comparison with experimental results on the critical fluid depth is therefore only possible by employing the double-dominant theory. The double-dominant theory (see Figs. 4 and 5) clearly shows a *soft-spring* branching for any $h \geq h_R$. This means that the experimentally determined critical depths should be much smaller than the theoretical value h_R. What is this value? Fultz[12] estimated it at $h_R^* = 0.28$. The difference between the theoretical value $0.3368\ldots$ and the experimental value 0.28 looks quite large and needs an explanation. The explanation can be given within the framework of the double-dominant theory. We should recall the experimental technique by Fultz[12] and take the fact into account that his laboratory experiments were done with small, but fixed values of τ.

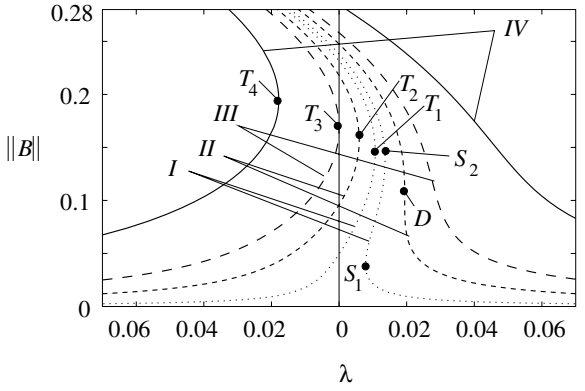

Fig. 7. Perturbed nonlocal branches at $\lambda = 0$ for $h = h_{R}* = 0.28$ (the experimental critical depth from laboratory experiments of Fultz) with different initial imperfections τ (forcing amplitude). The results for $\tau = 0.00002$ are represented by the dotted line, the results for $\tau = 0.000904$ by the line with small dashes, the results for $\tau = 0.0018388381$ by the line with long dashes and the results for $\tau = 0.005$ by the solid line. The points T_i, $i = 1, \ldots, 4$, denote the turning points on the left subbranch, the points S_1 and S_2 mark two turning points on the right subbranch, and the point D, which occurs for $\tau = 0.000904$, is a double turning point.

In order to show that the experimental critical depth is a function of τ, we present in Fig. 7 the perturbed nonlocal branching (by the double-dominant theory) for $h = h_R^* = 0.28$ and different values of τ. The smallest tested value of τ leads to a locally *hard-spring* behavior of the smallest $\|B\|$ at $\lambda = 0$. This result is consistent with the local solution presented in Sec. 4.1. Since the experimental technique by Fultz[12] was only able to detect the lowest stable resonant waves (solutions with the lowest $\|B\|$ for each λ), the experiments show a maximal response at $\lambda = 0.00789946575$ (abscissa of S_1), i.e. for the forcing frequency which is larger than the linear eigenfrequency. As usual, the positiveness of λ indicates a *hard-spring* behavior, i.e. the resonance is expected at a higher forcing frequency than σ_1.

Furthermore, increasing τ changes the branching. Two special cases are marked by dashed lines in Fig. 7. The two turning points S_1 and S_2 which are located on the nonlocal branches for the smallest τ pass into the double turning point D. In that case, the maximum amplitude in the tests is expected at the abscissa of T_2, i.e. for $\lambda = 0.00594460116$ (remembering that experiments can only detect solutions of the lowest norm for each fixed λ). This value of λ should report on the *hard-spring* behavior (the maximal amplitude is found for $\sigma > \sigma_1$). Continuing the increase of τ leads to the situation where all turning points on the right subbranch are eliminated and, for a certain $\tau = 0.0018388381$, the maximal experimental steady-state response will be at $\lambda = 0$. This occurs when the abscissa of the turning point T_3 becomes zero. In this case, the test should indicate the critical fluid depth. A larger τ, e.g. $\tau = 0.005$ in Fig. 7, leads to a *soft spring*-like branching. Therefore, the maximum response has to occur at the abscissa of point T_4, for a negative λ, namely, for a forcing frequency $\sigma < \sigma_1$.

Fultz[12] has carried out experiments with different forcing amplitudes. The mean value of τ was $\tau_{\rm m} = 0.002$. This result agrees well with our theoretically determined value $\tau = 0.0018388381$ (see Fig. 7), for which the double-dominant theory expects the maximum amplitude response at $\lambda = 0$.

7. Concluding Remarks

We showed that the use of the asymptotic, double-dominant modal theory (Model 2 by Faltinsen and Timokha[4]) makes it possible to describe the secondary resonance and the corresponding amplification of the second mode. Our analysis focuses on steady-state (periodic) solutions and a continuous frequency domain that covers two subdomains in which the second mode can be amplified. The first subdomain is associated with the primary resonance (it has been studied in Part I by a single-dominant model). The second subdomain is situated slightly away from the primary resonance. It is characterized by the secondary resonance in the hydrodynamic system. The phenomenon of the secondary resonance was studied by Ockendon *et al.*,[28,29] Feng,[9,10] Faltinsen and Timokha,[4,7] and Wu.[34] However, these authors did not present the nonlinear branching at the secondary resonance zone. The present paper analyzes this branching for the first time and establishes links to the branching at the primary resonance zone. Special emphasis is also placed on the case of the critical liquid depth-to-breadth ratio.

Faltinsen and Timokha[4] performed a wide series of numerical experiments to prove that Model 2 gives an adequate prediction of the steady-state waves when the forcing frequency is close to the lowest natural frequency. Our theoretical studies have implicitly confirmed that the main part of the *sloshing energy* is concentrated on the two natural modes. Moreover, Faltinsen and Timokha[4] showed that a significant amplification of subsequent higher modes, i.e. third, fourth etc. can only occur away from the primary resonance domain or in the case of small liquid depths. This fact is illustrated in Fig. 6 by increasing the amplitude response at the point $\lambda_0(2,2)$.

On the other hand, it is also of interest to see what happens when the contribution of the higher modes is studied by the adaptive modal systems (Model M) developed by Faltinsen and Timokha[4] or by the Perko-like multimodal technique. Looking at the results of numerical experiments by Faltinsen and Timokha[4] and La Rocca *et al.*,[18–20] one can also expect that these techniques will help us to describe and understand the branching behavior for values of the bifurcation parameter λ on the left of $\lambda_0(2,2)$. This is an interesting task which requires a sophisticated work on special numerical schemes.

Acknowledgment

This work was in part supported by the DFG. A.T. also acknowledges the sponsorship made by the Alexander-von-Humboldt Foundation.

References

1. H. N. Abramson, The dynamics of liquids in moving containers, NASA Report, SP 106, 1966.
2. P. J. Bryant, Nonlinear progressive waves in a circular basin, *J. Fluid Mech.* **205** (1989) 453–467.
3. O. M. Faltinsen, A nonlinear theory of sloshing in rectangular tanks, *J. Ship. Res.* **18** (1974) 224–241.
4. O. M. Faltinsen and A. N. Timokha, Adaptive multimodal approach to nonlinear sloshing in a rectangular rank, *J. Fluid Mech.* **432** (2001) 167–200.
5. O. M. Faltinsen and A. N. Timokha, Asymptotic modal approximation of nonlinear resonant sloshing in a rectangular tank with small fluid depth, *J. Fluid Mech.* **470** (2002) 319–357.
6. O. M. Faltinsen and A. N. Timokha, Analytically-oriented approaches to two-dimensional fluid sloshing in a rectangular tank (survey), in *Proc. of the Institute of Mathematics of the Ukrainian National Academy of Sciences: Problems of Analytical Mechanics and its Applications* **44** (2002) 321–345.
7. O. M. Faltinsen, O. F. Rognebakke and A. N. Timokha, Resonant three-dimensional nonlinear sloshing in a square base basin. Part 2. Effect of higher modes, *J. Fluid Mech.* **523** (2005) 199–218.
8. O. M. Faltinsen, O. F. Rognebakke, I. A. Lukovsky and A. N. Timokha, Multidimensional modal analysis of nonlinear sloshing in a rectangular tank with finite water depth, *J. Fluid Mech.* **407** (2000) 201–234.
9. Z. C. Feng, Transition to traveling waves from standing waves in a rectangular container subjected to horizontal excitations, *Phys. Rev. Lett.* **79**(3) (1997) 415–418.
10. Z. C. Feng, Coupling between neighboring two-dimensional modes of water waves, *Phys. Fluids.* **10**(9) (1998) 2405–2411.
11. P. Ferrant and D. Le Touze, Simulation of sloshing waves in a 3D tank based on a pseudo-spectral method, in *Proc. of 16th Int. Workshop on Water Waves and Floating Bodies*, Hiroshima, Japan (2001).
12. D. Fultz, An experimental note on finite-amplitude standing gravity waves, *J. Fluid Mech.* **13** (1962) 193–212.
13. M. Hermann, The numerical treatment of perturbed bifurcation problems in ordinary differential equations, *J. Comp. Appl. Math.* **9** (1983) 71–80.
14. M. Hermann and D. Kaiser, RWPM: A software package of shooting methods for nonlinear two-point boundary value problems, *Appl. Numer. Math.* **13** (1993) 103–108.
15. M. Hermann and K. Ullrich, RWPKV: A software package for continuation and bifurcation problems in two-point boundary value problems, *Appl. Math. Lett.* **5** (1992) 57–61.
16. M. Hermann and A. Timokha, Modal modelling of the nonlinear resonant fluid sloshing in a recnagular tank I: A single-dominant model, *Math. Mod. Meth. Appl. Sci.* **15** (2005) 1431–1458.
17. R. A. Ibrahim, *Liquid Sloshing Dynamics: Theory and Applications* (Cambrigde Univ. Press, 2005).
18. M. La Rocca, P. Mele and V. Armenio, Variational approach to the problem of sloshing in a moving container, *J. Theory Appl. Fluid Mech.* **1** (1997) 280–310.
19. M. La Rocca, G. Sciortino and M. A. Boniforti, A fully nonlinear model for sloshing in a rotating container, *Fluid Dyn. Res.* **27** (2000) 23–52.
20. M. La Rocca, G. Sciortino, C. Adduce, C. and M. Boniforti, Experimental and theoretical investigation on the sloshing of a two-liquid system with free surface, *Phys. Fluids* **17** (2005) 062101-1–062101-17.

21. M. Landrini, A. Colagorossi and O. M. Faltisen, Sloshing in 2-D flows by the sph method, in *Proc. of the 8th Int. Conf. on Numerical Ship Hydrodynamics*, Busan, Korea (2003).
22. R. Löhner, C. Yang and E. Onate, On the simulation of flows with violent free surface motion, *Comput. Meth. Appl. Mech. Eng.* **195** (2006) 5597–5620.
23. I. A. Lukovsky and A. N. Timokha, *Variational Methods in Nonlinear Dynamics of a Limited Liquid Volume* (Kiev, 1995), in Russian.
24. N. N. Moiseyev, To the theory of nonlinear oscillations of a limited liquid volume of a liquid, *Appl. Math. Mech.* (PMM) **22** (1958) 612–621, in Russian.
25. N. N. Moiseyev and V. V. Rumyantsev, *Dynamic Stability of Bodies Containing Fluid* (Springer, 1968).
26. R. E. Moore and L. M. Perko, Inviscid fluid flow in an accelerating cylindrical container, *J. Fluid Mech.* **22** (1964) 305–320.
27. J. R. Ockendon and H. Ockendon, Resonant surface waves, *J. Fluid Mech.* **59** (1973) 397–413.
28. H. Ockendon and J. Ockendon, Nonlinearity in fluid resonances, *Meccanica* **36** (2001) 297–321.
29. H. Ockendon, J. Ockendon and D. D. Waterhouse, Multi-mode resonance in fluids, *J. Fluid Mech.* **315** (1996) 317–344.
30. L. M. Perko, Large-amplitude motions of liquid-vapour interface in a accelerating container, *J. Fluid Mech.* **35** (1969) 77–96.
31. P. N. Shankar and R. Kidambi, A modal method for finite amplitude, nonlinear sloshing, *Pramana — J. Physics* **59** (2002) 631–651.
32. W. Wallisch and M. Hermann, *Numerische Behandlung von Fortsetzungs- und Bifurcationsproblemen bei Randwertaufgaben* (Teubner, 1987).
33. D. D. Waterhouse, Resonant sloshing near a critical depth, *J. Fluid Mech.* **281** (1994) 313–318.
34. G. X. Wu, Second-order resonance of sloshing in a tank, *Ocean Engineering*, in press.